

## Thermal fluctuation forces and wetting layers in colloid-polymer mixtures: Derivation of an interface potential

J. O. Indekeu,<sup>1</sup> D. G. A. L. Aarts,<sup>2</sup> H. N. W. Lekkerkerker,<sup>3</sup> Y. Hennequin,<sup>4</sup> and D. Bonn<sup>4,5</sup>

<sup>1</sup>*Instituut voor Theoretische Fysica, Katholieke Universiteit Leuven, Celestijnenlaan 200D, B-3001 Leuven, Belgium*

<sup>2</sup>*Department of Chemistry, Physical and Theoretical Chemistry Laboratory, University of Oxford, South Parks Road, Oxford OX1 3QZ, United Kingdom*

<sup>3</sup>*Van 't Hoff Laboratory, Utrecht University, Padualaan 8, 3584CH Utrecht, The Netherlands*

<sup>4</sup>*Van der Waals–Zeeman Institute, University of Amsterdam, Valckenierstraat 65, 1018XE Amsterdam, The Netherlands*

<sup>5</sup>*Laboratoire de Physique Statistique, Ecole Normale Supérieure, 24 Rue Lhomond, 75231 Paris Cedex 05, France*

(Received 20 November 2009; revised manuscript received 23 February 2010; published 28 April 2010)

We discuss wetting layers in phase-separated colloid-polymer mixtures adsorbed at a vertical wall, observed in recent laser scanning confocal microscopy experiments. Matching of colloid and solvent dielectric properties renders van der Waals forces negligible and provides a system governed by short-range forces and thermal fluctuations on which the subtle predictions of renormalization group (RG) theory for wetting can be tested. The width  $w$  of the fluid-fluid (“liquid-gas”) interface bounding the wetting layer scales with the square root of the wetting layer thickness  $\ell$ , in qualitative agreement with RG theory for short-range complete wetting in three dimensions. The measured wetting layer thickness  $\ell$  as a function of the height  $h$  above the horizontal plane of bulk phase separation is compared with two distinct theoretical predictions. A simple heuristic interface potential  $V(\ell)$ , first proposed in a previous report, is now fully derived, and confronted here with the interface potential based on the linear RG theory. The heuristic approach does not capture fully the RG treatment. While fundamental differences exist between the two approaches, the resulting predictions for  $\ell(h)$  are almost identical. However, the theory does not follow the precise shape of the experimental curve of  $\ell(h)$ .

DOI: [10.1103/PhysRevE.81.041604](https://doi.org/10.1103/PhysRevE.81.041604)

PACS number(s): 68.08.Bc, 82.70.Dd, 68.35.Ct, 68.37.-d

### I. INTRODUCTION

In this report we deal with fluctuation-induced forces that govern the thicknesses of wetting layers in the context of colloid-polymer mixtures. Background information on the system can be found in [1], where in particular it is explained how surface tensions and capillary lengths can be measured. A brief account of our experimental results and summary of the theoretical approach has been given in [2]. Our main present purpose is to give full detail of the derivation of the interface potential that was used in [2] to obtain a theoretical prediction for the thickness of the wetting layer adsorbed on the wall as a function of the height above the liquid-vapor interface.

The main characteristic of colloid-polymer mixtures is that the relevant physical scales are very different from what they are in molecular fluids. This provides extra opportunities for visualizing fluctuations and also for studying properties of fluctuations using the wetting theory for systems in three dimensions with *short-range forces*. This was considered to be a highly academic theory applicable to very few fluids of practical interest since the ubiquitous van der Waals forces are considered to be of long range (algebraic decay) in the field of wetting [3–5], as are the critical Casimir forces arising between a colloidal particle and a flat surface immersed in a near-critical liquid mixture [6].

Our discussion starts with a brief recollection of colloidal suspensions, followed by a specification of the interactions between the colloidal particles, which are to a good approximation hard spheres with tunable attractions emerging between them by adding polymers to the solvent. We proceed to address the important scales and introduce the main func-

tions and variables. Then we break the translational invariance by considering an adsorbing wall and discuss the wetting problem in a semi-infinite geometry. Subsequently we focus on the capillary wave fluctuations of a free interface, remote from any external confining wall, between liquidlike and gaslike phases. In the main part of the paper, we return to the confined system and study how the unbinding of the liquid-gas interface from the wall is affected by thermal fluctuations and how the subtle predictions of short-range wetting theory in  $d=3$  can be tested in this experimental system.

#### A. Colloidal suspension

Colloidal particles in suspension perform Brownian motion, driven by random collisions with solvent molecules according to the kinetic theory of heat. The suspension is stable against sedimentation as long as there is levitation by thermal agitation. This is the case if the thermal kinetic energy outweighs the gravitational potential energy, or in other words, if the thermal diffusion time is shorter than the sedimentation time. This is expressed by the inequality

$$\text{Pe} = (m_c - m_f)ga/k_B T < 1, \quad (1)$$

where the Peclet number  $\text{Pe}$  is the buoyant mass of the colloidal particle immersed in the fluid,  $m_c - m_f$ , times gravitational acceleration  $g$  and colloid radius  $a$ , divided by the thermal energy. For micron-sized colloids in suspension at room temperature  $\text{Pe} \approx 1$ , and its dependence on colloid radius is strong, since  $\text{Pe} \propto a^4$ . The colloidal particles in our system are fluorescently labeled poly(methyl methacrylate) of radius  $a=68$  nm. They are dispersed in a mixture of cyclohexyl bromide and decalin.

### B. Hard spheres+tunable attractions

The interactions between the colloids are strongly manipulated. Coating with adsorbing polymer first eliminates their mutual attraction and turns them into hard spheres. Van der Waals forces are suppressed by refractive index matching and static dielectric constant matching between colloid and solvent. Then nonadsorbing polystyrene polymers of radius of gyration  $R_g=71$  nm are added to the solvent, by which attractive forces are reintroduced, but now in a highly controllable manner and with a very simple functional dependence on colloid separation. The resulting pair potential allows fluid-fluid phase separation into a colloid-rich “liquid” and colloid-poor (polymer-rich) liquid called “gas,” with associated critical point in the Ising model universality class. Various theoretical approaches have been employed to study the rich phase behavior and structure of colloid-polymer mixtures [7].

The nonadsorbing polymer induces the well-known Asakura-Oosawa-Vrij depletion force [8–12] or entropic attraction between the colloids, which is proportional to the overlap volume  $V_o$  of zones around the colloids from which the polymers are excluded. This effect can also be understood as a result of the osmotic pressure  $\Pi$  of the polymers that squeezes nearby colloids together. The polymers are assumed to be of the same (effective) diameter or smaller than the colloids. The polymers are to a first approximation mutually *penetrable* spheres, so that they do not interact among their own kind and constitute an ideal gas. Polymers and colloids mutually interact like *impenetrable* hard spheres. The resulting attractive tail of the colloid-colloid pair potential, for a polymer density  $\rho_p^r$  (measured in a colloid-free solvent reservoir), is

$$U(r) = -\Pi V_o(r) = -\rho_p^r k_B T V_o(r), \quad (2)$$

where Van ’t Hoff’s ideal gas law for a dilute solution of polymers has been invoked in the second step. In the dilute limit the interaction energy is just the (average) number of polymers contained in the overlap volume, times  $k_B T$ . The strength (i.e., depth) of this monotonic attraction can be tuned by changing the polymer concentration and its short range can be manipulated by varying the polymer size  $R_g$ . The range is strictly finite, and approximately  $2(a+R_g)$ , since there is no interaction between colloids whose excluded zones do not overlap. Thus, a system of hard spheres with tunable short-range attractions results. Liquid-gas like coexistence and criticality should then be possible when the potential depth  $\epsilon$  is of order  $k_B T$ , and this is indeed observed.

### C. Scales

A first marked difference in *scales* between the colloid-polymer mixture and ordinary molecular liquids is that the liquid-gas interfacial tension  $\gamma$  is ultralow. Indeed, a rough estimate of the interfacial tension is the energy of a broken colloid-colloid bond, of order  $\epsilon \approx k_B T$ , per area  $a^2$ . Since  $a$  is about  $10^3$  atomic radii,  $\gamma$  is reduced by a factor of  $10^{-6}$  and falls in the nN/m range instead of mN/m. Second, the competition between the thermal wandering of the interface and the interfacial tension that aims at keeping the interface flat,

leads to a typical transverse displacement amplitude or thermal length  $L_T = \sqrt{k_B T / \gamma}$ , which is increased by a factor  $10^3$  and attains magnitudes up till  $\mu\text{m}$  instead of nm. Such large interface fluctuations can be studied directly using optical microscopy [13].

Third, the competition between interfacial tension and gravity is reflected in the capillary length  $L_{cap} = \sqrt{\gamma / g \Delta \rho}$ , which gives the longitudinal length scale over which an inclined interface can deviate from a horizontal plane. The inclination can be due to capillary rise near a wall or a long-wavelength capillary wave fluctuation.  $L_{cap}$  is typically  $10^3$  times smaller than what it is in molecular fluids, and is limited to  $\mu\text{m}$ , again due to the ultralow tension. Note that  $\Delta \rho$  is not very different from an ordinary liquid density. As a consequence, it is harder to resolve the contact angle and profile of the interface against a wall than it is for molecular fluids. Finally, also the times scales favor direct visual observation of capillary wave relaxation, since the capillary time  $\tau = (\eta / \gamma) L_{cap}$  is of the order of seconds as compared to  $10 \mu\text{s}$  for molecular fluids.

### D. Functions and variables

The main functions and variables can be identified as follows [14]. We consider  $N_c$  colloids in a volume  $V$  at temperature  $T$ , in contact with a reservoir of solvent and added polymer, through a semipermeable membrane which only prevents colloids from passing. Tuning the polymer chemical potential  $\mu_p$  in the reservoir allows to adjust the polymer concentration in  $V$ . This leads to a semigrand canonical potential

$$\Omega(T, V, N_c, \mu_p) = F_0(T, V, N_c) - \int_{-\infty}^{\mu_p} N_p(\mu_p') d\mu_p', \quad (3)$$

where  $F_0$  is the free energy of a system of  $N_c$  hard spheres, with no polymers present. An accurate expression can be obtained from the Carnahan-Starling equation of state [15]. Note that by invoking the ideal-gas approximation for the polymers and assuming low polymer activity this can be reduced to the appealing simple form  $\Omega(T, V, N_c, \mu_p) = F_0(T, V, N_c) - N_p(\mu_p) k_B T$ . In the so-called Free Volume Theory the number of polymers is estimated to be

$$N_p = n_p^r \alpha V, \quad (4)$$

where  $n_p^r$  is the reservoir polymer density and  $\alpha$  is the fraction of  $V$  that is accessible to the polymers. This fraction depends in a way determined by Scaled-Particle Theory on the colloid volume fraction  $\phi_c$  and the ratio of the depletion thickness  $\Delta$  and the colloid radius  $a$ . We have  $\alpha < 1 - \phi_c$ , and a crude estimate can be obtained by taking the dilute colloid limit (no overlap of excluded volumes),

$$\alpha \approx 1 - \frac{N_c}{V} \frac{4}{3} \pi (a + \Delta)^3, \quad (5)$$

with, for ideal polymers in bulk,  $\Delta \approx R_g$ . The polymer volume fraction,  $\phi_p$ , is related to its counterpart in the reservoir by

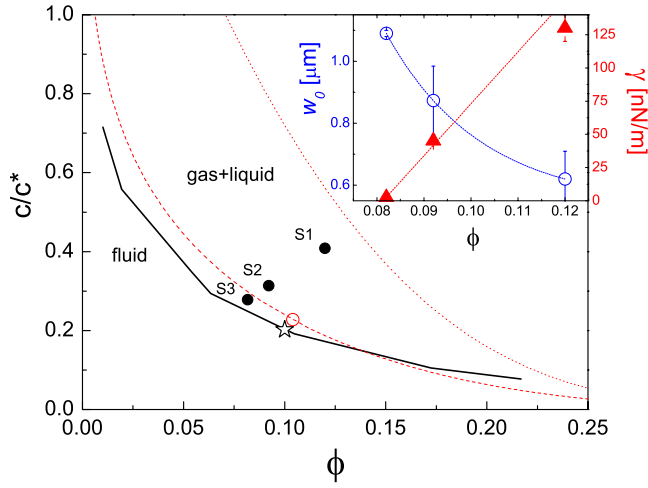


FIG. 1. (Color online) Phase diagram and interfacial properties of the colloid-polymer mixtures. The solid line is the experimental liquid-gas phase coexistence line for  $q=R_g/a=1.04$ .  $\phi$  is the colloid volume fraction  $\phi_c$  and  $c/c^*$  is the polymer concentration  $c$  relative to the overlap concentration  $c^*$ . Note that  $c/c^*=\phi_p$  if one assumes that the volume of one polymer coil is  $v_p=(4/3)\pi R_g^3$  with  $R_g$  the radius of gyration. The overlap concentration  $c^*$  is defined through  $\phi_p=1$ . The star marks the estimated location of the critical point. The state points studied are indicated as S1 ( $\phi=0.120$ ,  $c/c^*=0.408$ ), S2 (0.092, 0.314) and S3 (0.082, 0.278). The dashed line is the theoretical gas-liquid binodal for  $q=1$  from the Free Volume Theory (see Sec. I D). The (open) dot indicates the location of the theoretical critical point. The dotted line shows the corresponding theoretical wetting transition (see Sec. I E). Inset: Averaged width  $w_0$  (circles) and surface tension  $\gamma$  (triangles) of the free (liquid-gas) interface as a function of colloid volume fraction. Lines are guides to the eye.

$$\phi_p = \alpha \phi_p^r \quad (6)$$

Note that  $\phi_p^r$  is controlled directly by  $\mu_p$ . This free-volume approach can be refined by, for instance, taking into account that the polymers are not ideal balls but chains that interact with themselves and each other through excluded volume interactions. This allows polymers to attempt to wrap around colloids and this leads to a reduction of  $\Delta$ . We do not discuss this further here, but limit ourselves to pointing at the two main order parameters that emerge,  $\phi_c$  and  $\phi_p$ . The phase diagrams can be presented in terms of these two fractions, or in terms of the closely related ones  $\phi_c$  and the control variable  $\phi_p^r$ , for a given fixed size ratio  $R_g/a$ . Typical experimental paths in the phase diagram are dilution lines, which are straight lines through the origin in the  $(\phi_c, \phi_p)$  plane. The phase diagram, relevant to the systems we study, is shown in Fig. 1, which extends slightly the phase diagram shown in Fig. 1 of [2].

### E. Walls and wetting

The Young-Laplace equation, which gives us the thermodynamic contact angle  $\theta$  as a function of the surface free energies of the wall-gas, wall-liquid, and liquid-gas interfaces, describes the mechanical equilibrium of the three-phase contact line,

$$\gamma_{WG} = \gamma_{WL} + \gamma \cos \theta. \quad (7)$$

In order to explore the possibility of a wetting transition for this system, we can ask, for instance, how  $\theta$  varies with polymer concentration. (Note that the experiment is performed at fixed ambient temperature.) A wetting transition corresponds to a singularity in  $\cos \theta$ , whose value approaches 1 if the liquidlike phase is about to wet the wall, and sticks to 1 throughout the so-called complete wetting regime. If the singularity amounts to a discontinuity in the first derivative of  $\cos \theta$ , the transition is said to be of first order. If the first derivative is continuous, but a higher derivative is not, the transition is said to be critical. Critical wetting is an example of a *continuous* wetting transition. Another example of a continuous wetting transition is the approach to *complete wetting*, when the system is off of bulk phase coexistence but is tuned closer and closer to bulk coexistence by varying some control parameter termed *bulk field*, which in practice depends on the chemical potential(s).

A first approximation to calculating whether such transition occurs, is to employ the mean-field Cahn-Landau theory. The starting point of our analysis is the surface free-energy functional [16,17]

$$\begin{aligned} \chi[\rho] = & \int_0^\infty dz \left\{ f(\rho) - \mu_c \rho(z) + p_c + m(\rho) \left( \frac{d\rho}{dz} \right)^2 \right\} \\ & - h_1 \rho_1 - \frac{g}{2} \rho_1^2, \end{aligned} \quad (8)$$

which describes a colloid-polymer mixture adsorbed at a hard wall. In here,  $\rho(z)$  is the order parameter profile with  $z$  the perpendicular distance to the hard wall. The order parameter  $\rho$  is the *colloid* number density. A mean-field approach is adopted, in which the  $x$ - and  $y$ -dependence of  $\rho$  is neglected. We remark that it is not necessary to invoke a second density associated with the *polymer*, since in Free Volume Theory the latter depends on  $\rho$  and on the (fixed) polymer chemical potential. Thus there is just one independent density,  $\rho$ , which is proportional to  $\phi_c$ .

The functional  $\chi[\rho]$  consists of three parts: the first part of the integral is the contribution to the excess free energy per unit area from the pressure excess  $p_c - p(z)$ , where  $p(z) \equiv \mu_c \rho(z) - f(\rho)$ , with  $f(\rho)$  the bulk free-energy density of a homogeneous fluid of uniform density  $\rho$ . This part amounts to the familiar double well potential, the minimum of which describes the bulk equilibrium phase(s). The quantities  $\mu_c$  and  $p_c$  are the colloid chemical potential and pressure at two-phase coexistence of liquid and gas, respectively. It follows that the pressure excess vanishes in the coexisting bulk phases.

The second part in the integrand,  $m(\rho)(d\rho/dz)^2$ , is the leading term in an expansion in density inhomogeneities [18]. The coefficient of the squared gradient term is given by  $m(\rho) = \frac{\pi}{3} \int_0^\infty dr r^4 c(r, \rho)$  where  $c(r, \rho)$  represents the direct correlation function of Ornstein and Zernike with colloid center-to-center distance  $r$  and density  $\rho$ . We will approximate the direct correlation function by [19,20]

$$c(r, \rho) = \begin{cases} 0, & r \leq 2a \\ -\beta U(r), & r > 2a, \end{cases} \quad (9)$$

where  $U(r)$  is the attractive pairwise potential Eq. (2), and  $\beta=1/kT$ . This further simplifies calculations because it turns the coefficient  $m(\rho)$  into a constant  $m$ . Finally, the terms outside the integral reflect the contact interaction with the hard wall. Here  $\rho_1 \equiv \rho(0)$  is the contact density,  $h_1$  the surface field and  $g$  the surface enhancement [16]. Note that the wall-adsorbate interaction is also short ranged, in view of the matching of the dielectric properties of solvent and colloid, which greatly reduces the effective Hamaker constant of the wall-colloid interaction mediated by the solvent.

For our system,  $h_1 > 0$ , leading to a net attraction between the colloid-rich phase and the wall. This bias comes about because the overlap of excluded zones is greater between wall and colloid than between two colloids, for the same separation. The surface enhancement  $g < 0$  reflects that the colloid-colloid attraction is reduced near the wall with respect to what it is in bulk. This reduction is caused by the fact that the overlap of colloidal excluded zones also partly overlaps with the zone already excluded by the wall. The role of  $g$  is somewhat secondary to that of  $h_1$ . While  $h_1$  is responsible for inducing wetting by one of the phases (in our case the liquidlike phase), upon varying  $g$  the character of a wetting transition may change from first order to critical.

All the parameters entering in this Cahn-Landau theory can be identified for the colloid-polymer system and this theory predicts the possibility of a (first-order) wetting transition, which can occur farther from or closer to the bulk critical point depending on the value of the size ratio  $q = R_g/a$  [16] (see Fig. 1, dotted line, for  $q=1$ ). Although wetting transitions have been reported for similar adsorbed colloid-polymer mixtures [21], for the systems at hand only complete wetting has hitherto been observed experimentally [16]. Therefore, we have  $\theta=0$  and the liquid-gas interface merges tangentially with the (vertical) wetting layer adsorbed at the wall, as can be seen using laser scanning confocal microscopy (LSCM) (see Fig. 2 of [2]).

The properties we want to focus on are those of the wetting layer somewhat above the three-phase contact region, and in particular we are interested in the interface between that wetting layer and the adjacent gaslike phase in bulk. LSCM allows to obtain fluorescence intensity profiles versus depth  $z$  (the colloids being fluorescently labeled) from which the interface width and also the wetting layer thickness can be derived. Our main goals are (i) to interrelate these two lengths and (ii) to study the wetting layer thickness versus height.

### F. Free interface: Capillary wave roughness

Let's examine more closely the properties of the free and fluctuating liquid-gas interface now before we investigate further the effects of the wall-interface interaction. We will focus on interfacial tension effects and neglect bending rigidity, although the latter must be taken into account to describe accurately the full spectrum of interface fluctuations [22]. The horizontal free interface, far away from any wall but still

under the influence of gravity, can be described quite well by capillary-wave theory [23,24]. The thermally averaged height fluctuation squared is given by

$$\langle h(x, z)^2 \rangle \propto L_T^2 \ln \left[ \frac{\left(\frac{\pi}{a}\right)^2 + \left(\frac{1}{L_{cap}}\right)^2}{\left(\frac{\pi}{L_x}\right)^2 + \left(\frac{1}{L_{cap}}\right)^2} \right]. \quad (10)$$

Clearly, the thermal length  $L_T$  sets the amplitude of the fluctuations and the capillary length  $L_{cap}$  acts as a long-wavelength cutoff, preventing roughening at large parallel length scales. The parallel (horizontal) system size is  $L_x$ , and diverges in the thermodynamic limit. The colloid radius,  $a$ , acts as the short-wavelength cutoff. This is accurate as long as the system is not very close to the bulk critical point. Otherwise,  $a$  ought to be replaced by the bulk correlation length in the fluid,  $\xi$ , since then  $\xi > a$ . Indeed, capillary-wave theory assumes a self-affine interface (without overhangs), whereas on length scales between  $a$  and  $\xi$  overhangs cannot be neglected. In the following we stick to  $a$  for the time being, because it is a material constant of our system.

In the absence of gravity,  $L_{cap}$  diverges, and there is no damping of the fluctuations at large length scales. Consequently, the interface is *rough*, and we obtain

$$\langle h(x, z)^2 \rangle \propto L_T^2 \ln \left( \frac{L_x}{a} \right), \quad (11)$$

which diverges in the thermodynamic limit. In three dimensions this divergence is only logarithmic. This can be contrasted with the corresponding results for thermal interface wandering in lower dimensions  $d$  [25],

$$\langle h(x, z)^2 \rangle \propto L_T^2 \left( \frac{L_x}{a} \right)^{2\zeta}, \quad \text{with } \zeta = (3-d)/2, \quad (12)$$

where  $\zeta$  is the *roughness exponent* for thermal fluctuations in  $d \leq 3$ . Thus, the interface roughness in  $d=3$ , ignoring gravity, is very subtle, or “marginal,” since the (usual) power-law divergence turns into a logarithm.

### G. Interface unbinding from a vertical wall

For the vertical interface between the adsorbed wetting layer and the bulk “gas,” we can describe the positional fluctuations  $\Delta z = z(x, y) - \ell$ , about a vertical reference plane, at given average position  $z = \ell$ , by the following adaptation of Eq. (10),

$$\langle \Delta z(x, y)^2 \rangle \propto L_T^2 \ln \left( \frac{\xi_{\parallel}}{a} \right), \quad (13)$$

where the length scale  $\xi_{\parallel}$ , which now replaces the cutoffs  $L_x$  or  $L_{cap}$ , has nothing to do with the system size or the capillary length (which plays only a secondary role now that the direction of gravity is parallel to the interface). In contrast,  $\xi_{\parallel}$  is a consequence of a “wall potential,” which confines the interface fluctuations to some channel, or band. The largest parallel distance over which interface wandering is correlated, is by definition the *longitudinal* correlation length  $\xi_{\parallel}$ .

Typically, the interface transversally explores the width of the band, called *transverse* correlation length  $\xi_{\perp}$ , over a longitudinal length  $\xi_{\parallel}$ . Note that  $\xi_{\perp}^2 \equiv \langle \Delta z(x, y)^2 \rangle$ . If the effective wall potential would be just a hard boundary at  $z=0$  these explorations would bring the interface occasionally back to the wall, and  $\xi_{\parallel}$  would then be the typical distance along the wall between such collisions. In such case we would have  $\xi_{\perp} \approx \ell$ , signifying rather strong fluctuations.

The knowledge of the wall potential allows to obtain the wetting layer thickness  $\ell$  as a function of height. Good agreement between theory and experiment on vertical wetting layer thicknesses controlled by van der Waals forces was already demonstrated in early seminal work [26].

As was outlined in [2], to observe the vertical wetting layers against a glass wall a suitable LSCM setup was employed. The measurements were performed for three different state points S1, S2, and S3 for the colloid-polymer mixture with size ratio  $R_g/a=1.04$  described earlier. We first characterize the free interface and measure surface tension, density difference between the two phases and interfacial width. The surface tension  $\gamma$  and density difference  $\Delta\rho$  are found from the height-height correlation of the capillary fluctuations as described in [13]. The interfacial width  $w$  is deduced by fitting averaged fluorescence intensity profiles along the vertical  $y$  axis to the form

$$\bar{I}(y) = \frac{I_L - I_G}{2} \operatorname{erf}\left(\frac{y - y_0}{w\sqrt{2}}\right) + \frac{I_L + I_G}{2}, \quad (14)$$

with  $y_0$  the average position of that interface, and with  $I_L$  and  $I_G$  the average fluorescence intensities of the liquid and gas phases, respectively. We find surface tensions ranging from 130 (S1), 45 (S2) to 2.5 nN/m (S3) and with density differences of approximately 40, 27, and 4 kg/m<sup>3</sup>, respectively. The width of the *free* interface, denoted by  $w_0$ , is typically of the order of 1  $\mu\text{m}$  (see Fig. 1, inset). In general, the width  $w$  of a confined interface is defined through a profile described by an expression similar to Eq. (14) [2].

## II. INTERFACE WIDTH VERSUS WETTING LAYER THICKNESS: RG PREDICTION

Since the contributions from van der Waals forces are negligible for our system, forces between surfaces decay exponentially on the scale of the (micron-sized) bulk correlation length  $\xi$  and wetting theory for short-range forces (SRF) should apply [27,28]. For the Ising universality class, the wetting parameter

$$\omega = \frac{k_B T}{4\pi\gamma\xi^2}, \quad (15)$$

takes the value  $\omega \approx 0.8$  close to bulk criticality [29,30]. For state point S3 this value implies a bulk correlation length of magnitude  $\xi/a \approx 6$ , while for state points S2 and S1, the values are  $\xi/a \approx 1.4$  and 0.83, respectively. Renormalization group (RG) theory for *complete wetting* [28] predicts for  $\omega < 2$  the following relation between the wetting layer thickness  $\ell$  and the parallel correlation length  $\xi_{\parallel}$ , which is a measure of the average distance between interface bumps,

$$\ell/\xi \sim (2 + \omega)\ln(\xi_{\parallel}/\xi), \quad (16)$$

asymptotically for  $\ell/\xi \gg 1$ .

On the other hand, capillary-wave theory [23,24] predicts the following relation between the interfacial width  $w$  (or perpendicular correlation length  $\xi_{\perp}$ ) and  $\xi_{\parallel}$ ,

$$\xi_{\perp}^2 = \frac{k_B T}{2\pi\gamma} \ln\left(\frac{q_{\max}}{q_{\min}}\right) \equiv w^2, \quad (17)$$

where  $q_{\min} = \pi/\xi_{\parallel}$  and  $q_{\max} = \pi/a$  with  $a$  the particle radius. We recall that  $a$  ought to be replaced by the bulk correlation length  $\xi$  whenever  $\xi > a$ . Note that  $w$ , implicitly defined in Eq. (14), and  $\xi_{\perp}$  are both by definition equal to the root-mean-squared height fluctuation of the interface. Using Eq. (15), Eq. (17) can be written compactly as

$$\xi_{\perp}^2 = 2\omega\xi^2 \ln(\xi_{\parallel}/a). \quad (18)$$

Combining the RG expression (16) with the capillary-wave relation Eq. (17) leads to the important result that the mean-squared width of the confined interface depends *linearly* on the wetting layer thickness. For large  $\ell/\xi$ ,

$$w^2 \sim f(\omega)(k_B T/\gamma)^{1/2}\ell, \quad (19)$$

with  $f(\omega) = (\omega/\pi)^{1/2}/(2 + \omega)$  for  $\omega < 2$ .

A similar divergence of  $w^2$  as a function of  $\ell$  was already predicted, for all fluctuation regimes, in the early RG theory for short-range *critical wetting* in  $d=3$  [27]. The follow-up RG results for *complete wetting* transitions [28] implied that this behavior is valid more generally for all short-range continuous wetting transitions in  $d=3$ . This fact was highlighted when experiments on polymer mixtures and simulations in the 3d Ising model started to focus on size effects on interfacial widths in confined thin films [31]. In this context, Kerle, Klein, and Binder considered a confined system between opposing walls (one wall is perfectly wet and the other dry) a distance  $D$  apart, so that the film is in the soft-mode phase [32]. They derived the relation [33]

$$w_{KKB}^2 = 4\xi^2 + \frac{\pi\omega}{1 + \omega/2} \frac{\xi D}{4}, \quad (20)$$

which for large  $D$  fully agrees with Eq. (19) for large  $\ell$ , after careful identification of  $w_{KKB}$  with  $\sqrt{\pi/2}w$  and of  $D/2$  with  $\ell$ . The former identification follows from comparing Eq. (8) in [33] with our Eq. (14), and the latter is trivial. Note that the first term of Eq. (20) describes how  $w_{KKB}$  approaches an intrinsic microscopic width for small  $D$ .

We now proceed to check Eq. (19), valid for large  $\ell$ , or, equivalently, the asymptotic behavior for large  $D$  of Eq. (20), against the results of the measurements. The data points and the theoretical predictions (dashed curves) are shown in Fig. 2, which extends Fig. 3 of [2] in that also the theoretical curves for S1 and S2 are presented. Clearly, there is qualitative agreement between theory and experiment for the experimental system S3, which is closest to the bulk critical point. For S1 and S2 the measured values of  $w$  do not show a clear dependence on  $\ell$ , but nevertheless they are compatible, at least for S2, with the theoretical curves. In all cases, the measured interface widths are consistent with the general

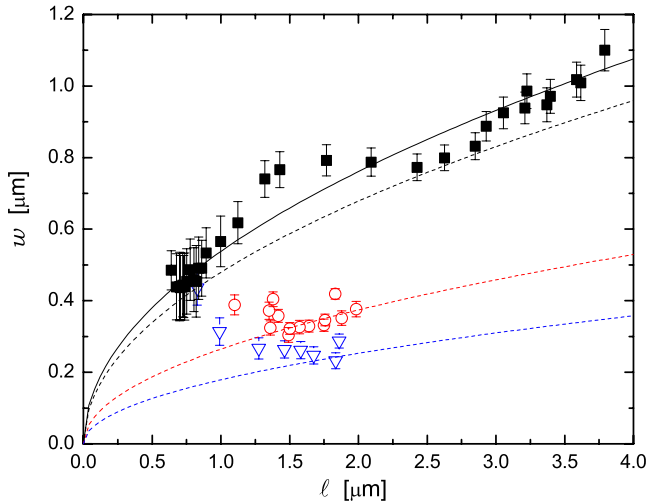


FIG. 2. (Color online) Measured width  $w$  of the interface between the wetting layer and the bulk “gas” phase, versus the wetting layer thickness  $l$ , for mixtures S3 (top; squares), S2 (middle; circles), and S1 (bottom; down triangles). The data are compared with the RG theory prediction, Eq. (19), assuming  $\omega=0.8$ , and using the measured interfacial tensions  $\gamma=130$  nN/m (S3), 45 nN/m (S2), and 2.5 nN/m (S1). The theoretical curves (dotted lines) are drawn for S3 (third from bottom), S2 (second from bottom) and S1 (bottom), and assume  $\omega=0.8$ . For S3 it is possible to obtain a meaningful fit to the data assuming the square-root dependence of  $w$  on  $l$  predicted by Eq. (19), with adjustable amplitude. The result is the topmost solid curve.

notion that fluctuations are hindered by confinement, since the widths are smaller than the corresponding values  $w_0$  for the free interface (cf. Fig. 1).

The predicted square-root dependence of  $w$  on  $l$ , Eq. (19), can be meaningfully fitted to the data for S3. This leads to  $w^2 \approx 0.29 \pm 0.05 \mu\text{m}l$ . The calculation, using  $\gamma \approx 2.5$  nN/m and no adjustable parameter, leads to  $w^2 \approx 0.23 \mu\text{m}l$ , in good qualitative agreement with the experiment. To substantiate this claim, we test the sensitivity of the amplitude,  $w^2/l$ , to changes in the wetting parameter  $\omega$ . Note that  $\omega$  is the only unknown parameter in our system because we have not measured the bulk correlation length  $\xi$  in the colloidal liquid. We have assumed the Ising model value for  $\omega$  at bulk criticality, which is approximately 0.8. Suppose now that this estimate is strongly perturbed, e.g., by a factor of 2. If  $\omega$  is taken to be 1.6, the calculated amplitude increases by 10%, from 0.23 to 0.25  $\mu\text{m}$ . In fact, the maximum increase that can be achieved is found for  $\omega=2$  (since  $f(\omega)$  is constant for  $\omega \geq 2$  [28]), and amounts to 11%. On the other hand, if  $\omega$  is lowered to 0.4, the amplitude decreases by 17%, to 0.19  $\mu\text{m}$ . We conclude that the theoretical ampli-

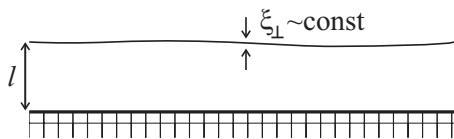


FIG. 3. Mean-field regime:  $\xi_{\perp}$  remains constant while  $l$  and  $\xi_{\parallel}$  diverge.

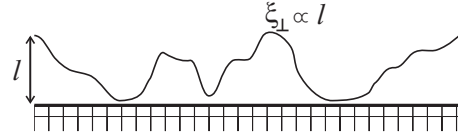


FIG. 4. Fluctuation regimes:  $\xi_{\perp} \propto l$ .

tude is not very sensitive to the value of  $\omega$  and that increasing  $\omega$  leads to a more favorable agreement between the theoretical and experimental amplitude, the result of the best fit being slightly larger than the maximal theoretical value. Note that, already for  $\omega=0.8$ , theory and experiment agree within the error margin including the rather large “oscillation” of the data about a simple square-root behavior.

Prior to our experiments, a first observation of an increase of the interfacial width with film thickness was made in a phase separated binary mixture of random copolymers [31]. The increase of  $w$  with  $l$  was found to be quasilinear, in crude agreement with three-dimensional Ising model simulations which showed a clear square-root dependence of  $w$  on  $l$  [31]. In the experimental system the presence and possible importance of long-range van der Waals forces, for which a logarithmic dependence of  $w$  on  $l$  is predicted, as well as other effects were invoked to explain the differences between the observations and the pure square-root dependence predicted for short-range forces [33].

In closing this section, we stress that a square-root dependence of  $w$  on  $l$  is quite special. It represents a border line case between two main regimes [25,34]. The first one is the mean field or smooth interface regime (Fig. 3), for which  $w$  saturates to a constant as a function of  $l$ , for large  $l$ , or diverges very weakly (e.g., logarithmically). Systems with van der Waals forces in  $d=3$ , and, more generally, systems above the upper critical dimensionality  $d_u$  for interface fluctuations fall in this class. The second one is the rough interface regime (Fig. 4) and contains all systems in  $d < d_u$ , which are characterized by important thermal fluctuations and interface displacements which “frequently” hit the wall, so that, naturally,  $w \propto l$ . We recall that  $d_u=3$  for short-range forces and  $d_u < 3$  for forces with algebraic decay. The case of membranes in  $d=3$  is also included in the category  $w \propto l$  [34]. In conclusion, an intermediate behavior (Fig. 5) of the form  $w \propto l^p$ , with  $0 < p < 1$  is untypical. Nevertheless, the power  $p=1/2$  is universal in its own right, since it holds for all fluctuation regimes and for critical and complete wetting alike, provided the forces are of short range and provided  $d=3$ .

### III. FLUCTUATION-INDUCED INTERFACE POTENTIAL: SIMPLE PICTURE

For interfaces bound to a wall by an attractive mean-field potential, interface fluctuations modify the wall-interface

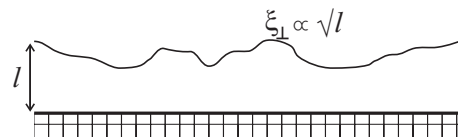


FIG. 5. Marginal regime:  $\xi_{\perp} \propto \sqrt{l}$ .

forces. For instance, the fact that (long-wavelength) interface fluctuations are hindered by the wall leads to a decrease in interfacial entropy, and thus an increase in interfacial free energy, of the confined interface as compared to one that is free [35,36]. The confinement of the fluctuations is therefore a relevant contribution to a fluctuation-induced disjoining pressure  $\Pi_{fl}(\ell)$  which repels the interface from the wall. The disjoining pressure is related to the associated interface potential  $V_{fl}(\ell)$  through  $\Pi_{fl}(\ell) \equiv -dV_{fl}(\ell)/d\ell$ . This contribution competes with the mean-field term (of, e.g., gravitational origin) which binds the interface.

To clarify the origin and form of the various physically plausible contributions to  $V_{fl}(\ell)$  we adopt the simple phenomenological picture proposed by Lipowsky and Fisher [34,37]. This heuristic approach is based on standard scaling assumptions concerning energy and entropy contributions of interface fluctuations, and for a variety of forces it correctly describes the mean-field critical behavior ( $d > d_u$ ) and the so-called weak-fluctuation critical behavior ( $d$  just below  $d_u$ ) [37]. Following this line of reasoning we arrive at an approximate interface potential which can be directly confronted with the experimental data. For short-ranges forces, however, various distinct fluctuation regimes exist precisely at  $d = d_u = 3$ , and the heuristic approach leads to a form for  $V_{fl}(\ell)$  that is different from that obtained by the standard (linear) functional RG approach [27]. That is why, in the next section, we compare our results based on the “simple-picture” interface potential with those using the RG interface potential as input.

As usual the starting point is the interface displacement model featuring an effective Hamiltonian for interfacial configurations  $\ell(\mathbf{x})$ ,

$$\mathcal{H}[\ell] = \int d^{d-1}x \left\{ \frac{1}{2} \gamma (\nabla \ell)^2 + V_w(\ell) \right\}. \quad (21)$$

The first term in the integral represents the elastic free energy of the interface and the second one gives the direct wall-interface interaction free energy. The surface free energy difference between a bound and a free interface is then argued to consist of three parts [37]: (i) a direct interaction term  $V_w(\bar{\ell})$ , which can be interpreted as the mean-field free energy for a wetting layer of mean thickness  $\bar{\ell}$ , (ii) the elastic energy associated with the increased area of a bent interface which is of order  $\gamma (\nabla \ell)^2 \approx \gamma \xi_{\perp}^2 / \xi_{\parallel}^2$  since the interface makes a typical transverse displacement  $\xi_{\perp}$  on a longitudinal length scale  $\xi_{\parallel}$ , and finally (iii) the entropy loss due to the confinement of interface fluctuations to a slab of typical width  $\xi_{\perp}$  (see Fig. 3 in [37]). “Collisions” of the interface with the boundaries of this slab reduce the entropy by an amount  $k_B$  per area  $\xi_{\parallel}^{d-1}$ , in accord with the equipartition theorem. These latter two contributions (ii) and (iii) are assumed to add up, in  $d=3$ , to the total *fluctuation* interface potential  $V_{fl}(\xi_{\perp}, \xi_{\parallel})$ ,

$$V_{fl}(\xi_{\perp}, \xi_{\parallel}) = (\gamma \xi_{\perp}^2 + k_B T) / \xi_{\parallel}^2. \quad (22)$$

Using  $\xi_{\perp} \equiv w$  and relation Eq. (17) which allows to express  $\xi_{\parallel}$  as a function of  $\xi_{\perp}$ , we get

$$V_{fl}(w) = \frac{(\gamma w^2 + k_B T)}{a^2} \exp\left(-\frac{4\pi\gamma w^2}{k_B T}\right), \quad (23)$$

which is Eq. (3.36) in [37]. In order to obtain an explicit dependence on the layer thickness, we further *assume* that  $w$  is related to the mean thickness  $\bar{\ell}$  through the RG result Eq. (19). This leads to our final form

$$V_{fl}(\bar{\ell}) = \frac{(\gamma b \bar{\ell} + k_B T)}{a^2} \exp\left(-\frac{4\pi\gamma b \bar{\ell}}{k_B T}\right), \quad (24)$$

where  $b \equiv f(\omega)(k_B T / \gamma)^{1/2} = [2\omega / (2 + \omega)] \xi$  is the proportional-ity constant between  $w^2$  and  $\ell$  in Eq. (19).

A number of comments are in order at this point. The main characteristic of this fluctuation interface potential is the *exponential decay* for large  $\bar{\ell}$ . This is physically correct for our system, and the decay constant is identical to that predicted by RG theory (see next Section). In this respect our potential is very different from the *Gaussian* potential applicable to systems with added surfactants in which the interface has negligible interfacial tension but significant bending rigidity [38]. On the other hand, the presence of a term linear in  $\bar{\ell}$  in the prefactor of the exponential is *not* a robust physical feature, but rather depends sensitively on our *ad hoc* assumptions. This linear term seems to come from the scaling assumptions for the elastic energy, which slightly dominates the entropic repulsion contribution in  $d=3$  [34]. But note that such linear terms, or other powers of  $\bar{\ell}$ , can also arise from possible logarithmic correction terms to Eq. (19), when Eq. (19) is substituted in Eq. (23). We shall see shortly that no such linear term is generated in the RG theory.

The total interface potential, from this simple picture, comes out as

$$V(\bar{\ell}) = V_w(\bar{\ell}) + V_{fl}(\bar{\ell}). \quad (25)$$

We take the wall potential appropriate for short-range forces and complete wetting transitions,

$$V_w(\bar{\ell}) = \Delta\rho g h \bar{\ell} + A \exp(-\bar{\ell}/\xi). \quad (26)$$

The first term in  $V_w$  is an attractive and linear part reflecting the undersaturation of the gas phase in bulk at a height  $h$  above the horizontal liquid-gas interface. For the time being we consider only configurations with *horizontal* interfaces, such as, e.g., a horizontal wetting layer suspended from a horizontal substrate at an elevation  $h$  above the bulk “liquid” reservoir. The second term (with  $A > 0$ ) is the short-range repulsion, which induces complete wetting in the limit  $h \rightarrow 0^+$ . The amplitude  $A$  can in principle be calculated within a mean-field theory applied to our specific colloid-polymer system [16,17], but there is no need to do this yet. Indeed, the second term in  $V_w$  can be safely neglected if we limit our considerations to the *leading* repulsive part in  $V$ , which is the fluctuation-induced short-range repulsion contained in  $V_{fl}$ . The latter is of slightly *longer range* than the former, which can be seen most clearly by rewriting Eq. (24) as

$$V_{fl}(\bar{\ell}) = \frac{(\gamma b \bar{\ell} + k_B T)}{a^2} \exp\left(-\frac{2}{2 + \omega} \frac{\bar{\ell}}{\xi}\right). \quad (27)$$

The wetting parameter  $\omega \approx 0.8$  thus acts so as to weaken the exponential decay. Another way to appreciate this is to note the interesting equality, using Eq. (16) (with the substitution  $\ell \rightarrow \bar{\ell}$ ),

$$\exp\left(-\frac{2}{2 + \omega} \frac{\bar{\ell}}{\xi}\right) = \left(\frac{\xi_{||}}{\xi}\right)^\omega \exp\left(-\frac{\bar{\ell}}{\xi}\right), \quad (28)$$

which links the heuristic approach to the functional renormalization of the wall potential  $V_W$ , discussed in the next section. Clearly, the divergence of  $\xi_{||}^\omega$  at complete wetting ( $\bar{\ell} \rightarrow \infty$ ) in the manner  $\exp(\omega \bar{\ell} / (2 + \omega) \xi)$  partially opposes the decay of the repulsive part of the wall potential.

In sum, we keep only the most relevant terms in the interface potential and propose

$$V(\bar{\ell}) = \Delta \rho g h \bar{\ell} + V_{fl}(\bar{\ell}), \quad (29)$$

which is independent of the amplitude  $A$  featured in Eq. (26)! Minimizing this potential with respect to  $\bar{\ell}$  allows us, for instance, to obtain an approximation for the equilibrium thickness  $\ell$  of a uniform wetting layer on a *horizontal* substrate exposed to an undersaturated vapor. The chemical potential is shifted from its value at two-phase liquid-vapor coexistence by an amount proportional to  $gh$ . The result, previously presented without details of derivation in [2], is

$$\left[ (4\pi - 1) + \frac{4\pi\gamma b \ell}{k_B T} \right] \exp\left(-\frac{4\pi\gamma b \ell}{k_B T}\right) = \frac{\Delta \rho g h a^2}{\gamma b}, \quad (30)$$

which defines a function  $h(\ell)$ , which may be inverted to an explicit function  $\ell(h)$  by using a suitable branch of the Lambert  $\mathcal{W}$  or ‘‘product log’’ function.

Before proceeding towards an application to a *vertical* wetting layer, in Sec. V, we check the self-consistency of the heuristic approach. This will lead to a confrontation between the heuristic interface potential and the one derived from linear RG theory, which is briefly recalled in the next Sec. IV. For completeness, we also check the validity of the Gibbs adsorption equation for both approaches, heuristic and RG, and test the validity of hyperscaling. These two issues are dealt with in the Appendices A and B, respectively.

In order to examine the mutual consistency of capillary-wave result Eq. (18), RG result Eq. (19) and our interface potential Eq. (25), based on Eq. (24), we rewrite the pertinent contributions to our interface potential Eq. (25) in a transparent and dimensionless form,

$$V(\bar{\ell}) a^2 / k_B T = H \frac{\bar{\ell}}{\xi} + \left( c \frac{\bar{\ell}}{\xi} + 1 \right) \exp\left(-\kappa \frac{\bar{\ell}}{\xi}\right). \quad (31)$$

While the parameters  $H = \Delta \rho g h \xi a^2 / k_B T$ ,  $c = \gamma b \xi / k_B T$ , and  $\kappa = 2 / (2 + \omega) = 4\pi c$  are known explicitly for our interface potential, they can also, for the sake of generality of the following argument, be left unspecified and considered to be independent and free.

We derive  $\xi_{||}$  in the standard manner [28,37], through its connection with the curvature of the interface potential in its minimum,

$$\frac{\gamma}{\xi_{||}^2} \equiv \left. \frac{\partial^2 V(\bar{\ell})}{\partial \bar{\ell}^2} \right|_e. \quad (32)$$

This leads to

$$\frac{a^2}{k_B T} \frac{\gamma}{\xi_{||}^2} = -\frac{\kappa}{\xi^2} \left[ 2c - \kappa \left( c \frac{\ell}{\xi} + 1 \right) \right] \exp\left(-\kappa \frac{\ell}{\xi}\right) \quad (33)$$

from which we derive

$$\ell / \xi = \frac{2}{\kappa} \ln(\xi_{||} / \xi) + \mathcal{O}(\ln \ln(\xi_{||} / \xi)) \quad (34)$$

and, using capillary-wave theory relation Eq. (18), we obtain

$$\xi_{\perp}^2 = \omega \xi \kappa \ell + \mathcal{O}(\ln \ell). \quad (35)$$

Note that Eqs. (34) and (35) reproduce Eqs. (16) and (19) to leading order in  $\xi_{||}$  and  $\ell$ , respectively, *provided*  $\kappa = 2 / (2 + \omega)$ . In view of Eq. (27) our interface potential does satisfy this requirement and our approach is therefore self-consistent, *but only to leading order*. Note that the value of the coefficient  $c$  is irrelevant for the leading asymptotic behavior, but not for the next-to-leading one, indicated by the correction to Eq. (34). Such log-log correction is *not* present in the RG theory for  $\omega < 2$  [28], to which we now turn.

#### IV. INTERFACE POTENTIAL FROM RG THEORY

The functional RG theory for wetting renormalizes the bare interface potential so that thermal capillary wave fluctuations of the interface are taken into account. In its simplest form the RG approach can be understood in terms of a convolution of the bare potential with a Gaussian of width  $\xi_{\perp} \equiv w$ . One thus obtains

$$V_{RG}(\bar{\ell}) = \langle V_W(\bar{\ell}) \rangle = \Delta \rho g h \langle \bar{\ell} \rangle + A \langle \exp(-\bar{\ell} / \xi) \rangle, \quad (36)$$

where

$$\langle f(x) \rangle \equiv \frac{1}{\sqrt{2\pi w}} \int_0^\infty dx' f(x') \exp[-(x - x')^2 / 2w^2]. \quad (37)$$

The smearing, over a width  $w$ , does not modify the *form* of the potential provided the mean displacement  $\bar{\ell}$  is sufficiently large *and* the fluctuations do not bring the interface close to the wall; conditions which for our potential are fulfilled for  $\omega < 2$  [28]. The renormalized potential is then

$$V_{RG}(\bar{\ell}) = \Delta \rho g h \bar{\ell} + A \exp(w^2 / 2\xi^2) \exp(-\bar{\ell} / \xi), \quad (38)$$

which, using Eq. (18), can be written as

$$V_{RG}(\bar{\ell}) = \Delta \rho g h \bar{\ell} + A (\xi_{||} / a)^\omega \exp(-\bar{\ell} / \xi). \quad (39)$$

In the second term we recognize the form Eq. (28) found in the heuristic approach. The (only) formal difference between the RG potential and the heuristic one is that in the former

the amplitude of the exponential repulsion is *independent* of  $\bar{\ell}$ .

The equilibrium wetting layer thickness  $\ell$  is obtained by minimizing  $V_{RG}(\bar{\ell})$  with respect to  $\bar{\ell}$ , and  $\xi_{\parallel}$  is obtained through Eq. (32), as usual. The two results combined imply Eq. (16) up to a constant correction. There is no logarithmic correction of log-log form. Therefore we also obtain Eq. (19) without logarithmic correction. We can further combine these relations to find  $\ell(h)$ ,

$$\exp\left(-\frac{2}{2+\omega}\frac{\ell}{\xi}\right) = \frac{(2+\omega)\Delta\rho g h \xi}{2A}, \quad (40)$$

which can be written in a form which allows easy comparison with Eq. (30),

$$4\pi \exp\left(-\frac{4\pi\gamma b\ell}{k_B T}\right) = \frac{\Delta\rho g h k_B T}{\gamma b A}, \quad (41)$$

where  $A$  is an as yet undetermined parameter. The same result follows if one first substitutes the  $\ell$  dependence of  $\xi_{\parallel}$  into Eq. (39) before minimizing the potential. The present approach is fully self-consistent.

In sum, the RG approach leads to a simple multiplicative renormalization of the exponential repulsion that can be calculated in the Cahn-Landau (mean-field) theory of wetting for colloid-polymer mixtures [16]. It suffices, in that mean-field theory, to rescale the bulk correlation length  $\xi$  to  $(2+\omega)\xi/2$  in order to obtain the RG prediction for  $\ell(h)$  in the weak-fluctuation regime  $\omega < 2$ . In order to get a quantitative interface potential, the mean-field amplitude  $A$  is to be calculated explicitly. This issue will be addressed in the next section.

## V. WETTING LAYER THICKNESS VERSUS HEIGHT

The relation(s) we derived between wetting layer thickness and height can serve to determine the profile of a *vertical* wetting layer, in the complete wetting regime, provided a few precautions are respected [3]. First, the elevation  $h$  above the horizontal liquid-gas interface should well exceed the capillary length  $L_{cap}$  in order for curvature contributions of order  $\gamma d^2 \ell / dh^2$  to be negligible compared to the disjoining pressure and gravitational pressure terms. This defines the so-called *film regime* [3]. Second, the approximation we make breaks down above a finite height  $h_m$  for which  $\ell(h_m) = 0$ . Above  $h_m$  a microscopic film may still exist, which is not described by the continuum theory at hand. This theory assumes that the colloid density is a smooth function, so that structure on length scales smaller than the bulk correlation length may be ignored.

While our phenomenological and heuristic interface potential leads to a function  $\ell(h)$  which can be confronted directly with experimental data, the RG interface potential approach still requires fixing the unknown parameter  $A$  by means of a full (mean-field) Cahn-Landau calculation. A precise determination of this amplitude was recently performed, for a colloid-polymer system with size ratio  $R_g/a=1$  and for a polymer concentration corresponding to a first-order wetting transition [17]. Since for us  $R_g/a=1.04$  and since we

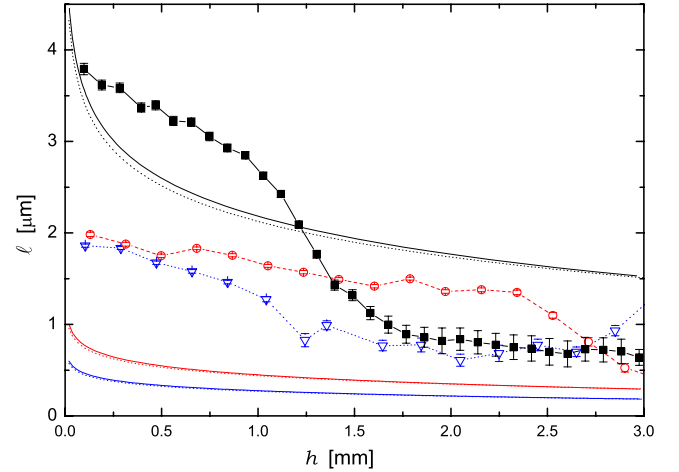


FIG. 6. (Color online) Comparison between the measured wetting layer thicknesses  $\ell$  for mixtures S3 (squares), S2 (circles), and S1 (down triangles) as a function of height  $h$  and theoretical predictions for  $\ell(h)$  based on the heuristic interface potential (smooth solid curves) and the linear RG interface potential (smooth dotted curves). The lines connecting the experimental data are merely guides to the eye. The theoretical curves are for S3 (top), S2 (middle), and S1 (bottom). The theoretical solid and dotted curves, for a given mixture, are almost coincident on this scale.

consider the complete wetting regime (which starts at the wetting transition), it is fully adequate that we make use of the results of these computations, in particular that for  $A$ , which reads,

$$A \approx 1.214 k_B T / (\pi a / 3)^2 \approx 1.11 k_B T / a^2. \quad (42)$$

When this is inserted in Eq. (41) comparison with Eq. (30) teaches us that the heuristic  $\ell(h)$  and the one obtained through RG theory differ formally only by the presence of the extra term linear in  $\ell$  in the prefactor of the exponential in the left hand side of Eq. (30). The constant in this prefactor turns out to be nearly the same in the two approaches ( $4\pi-1$  versus  $1.11 \times 4\pi$ , the relative difference being only 20%). To see how important is the difference between the two alternative theoretical expressions for  $\ell(h)$ , we plot them, together with the measured data. This is done in Figure 6. The two curves are almost coincident, for each system considered (S1, S2, and S3). Further, testing the sensitivity of the calculated curves with respect to the value of  $\omega$ , for S3, we find that the curves move slightly further apart when, in the factor  $f(\omega)$  in the expression for  $b$ ,  $\omega$  is lowered from 0.8 to 0.6, while they move closer together, cross each other, and move slightly apart when  $\omega$  is increased from 0.8 to 1. In this window of  $\omega$ ,  $0.6 < \omega < 1$ , the difference between the curves, e.g., at  $h=1$  mm, does not exceed 4 times the small difference perceptible in Fig. 6 (top curves), which is computed for  $\omega=0.8$ .

While, for all our systems (S1, S2, and S3), the difference between the two theoretical approximations is too small to merit concern, the agreement with experiment is not satisfactory. For S3, the data display two distinct regimes, above and below  $h \approx 1.2$   $\mu\text{m}$ , while the theory predicts a single regime. Speculations on possible explanations for this were presented

in [2]: It is likely that for S3 the equilibrium layer thickness was not reached yet despite resting times of up to several days before measurements were performed. In fact, the equilibration times for wetting films can be rather long [39], especially in these systems for which transport is governed by diffusion processes. However, it is important here to stress that the relaxation time scale for the capillary fluctuations is comparatively very short [13] and that the measured  $\ell$  dependence of the interface width  $w$  should be unaffected.

For the systems farther from the critical point, S1 and S2, it should be noted that the behavior of  $l$  versus  $h$  is more “regular,” displaying just a single regime more compatible with a simple logarithmic dependence. However, the experimentally observed thicknesses are much larger than the theoretical ones. This is not really surprising, since for S1 and S2 the interfacial tension  $\gamma$  is much larger than for S3. Consequently, assuming that  $\omega$  does not change appreciably when moving towards S2 and S1 and thus keeping  $\omega=0.8$ , since the increase in  $\gamma$  is accurately compensated by the decrease in  $\xi^2$  (as long as the system is not too far from the critical point), the fluctuation contribution to the disjoining pressure is several orders of magnitude smaller than the gravitational contribution, at wetting layer thicknesses comparable to the measured ones. Therefore, for S1 and S2 it is not plausible that the rather large observed wetting layer thicknesses are stabilized by interface fluctuations. The observed layer thicknesses for S1 and S2 thus remain unexplained, while those for S3 can be accounted for (in overall magnitude) by assuming interface fluctuation repulsion as the dominant force balancing gravitational thinning.

## VI. CLOSING REMARKS

In this note we attempted to clarify, and to put in a broader context, the theoretical approach adopted in analyzing the experimental data of [2]. Concerning the main issue of the dependence of the width or roughness  $w$  of the wetting layer interface on the wetting layer thickness  $\ell$ , there is qualitative agreement between the RG predictions for wetting with short-range forces in  $d=3$  and the experimental data.

Further, a heuristic approach without adjustable parameters, based on a phenomenological simple picture advocated by Lipowsky and Fisher, leads to a fluctuation interface potential which has the generally expected exponential decay with suitable renormalized range. The amplitude of this exponential contains a constant and a term linear in the wetting layer thickness  $\ell$ . Although the physical origin of this term linear in  $\ell$  is at first sight transparent, as it comes directly from the elastic energy cost of a deformed interface, the (asymptotic) self-consistency of the heuristic approach does not extend far enough to allow control of the coefficients of powers of  $\ell$  in front of the exponential decay.

The RG approach, on the other hand, is fully self-consistent. Further, it requires extra input from the mean-field theory in order to quantify the amplitude of the bare potential which is being renormalized. The RG calculation does not generate the term linear in  $\ell$  encountered in the amplitude of the exponential in the heuristic approach. The

*ad hoc* scaling ansatz and the RG are thus in mutual disagreement on this point, but on the more important aspects such as the exponential form and its proper decay length, both approaches agree.

The problem of the possible presence of polynomial prefactors of exponentially decaying terms in the interface potential for short-range critical (or complete) wetting has an interesting history [40]. A new development based on *nonlocal* interfacial models, by Parry *et al.*, has led to the insight that, for full thermodynamic consistency, any polynomial prefactor to an  $\exp(-n\kappa\ell/\xi)$  term in  $V(\ell)$  has to be of degree  $n-1$  [41]. The heuristic interface potential does not satisfy this constraint, since the prefactor is of degree  $n$  (with  $n=1$ ), while the linear RG interface potential passes the test.

In conclusion, the two theoretical approaches we discussed differ in important ways when judged from a fundamental point of view. Nevertheless, the resulting predictions for the wetting layer thickness  $\ell$  versus height  $h$  are almost identical, at least for the particular system under study. The predicted  $\ell(h)$  is of the same order of magnitude as the experimentally measured layer thicknesses, for system S3, which is close to the bulk critical point. However, the experimental data for S3 show an extra structure which cannot be captured by simple (quasi-)logarithmic forms for  $\ell(h)$ . For S2 and S1, farther from the critical point, the theoretical  $\ell(h)$  is significantly smaller than the measured one. Clearly, the measured layer thicknesses cannot be understood as being stabilized by interface fluctuations alone. In sum, for S3 as well as for S2 and S1, essential features yet remain unexplained in the theory and/or the experiment.

## ACKNOWLEDGMENTS

We thank Andrew Parry and Bob Evans for very stimulating critical comments on the theoretical part of [2] and for detailed helpful comments on the present manuscript. Without their incentive the necessity of a scrutiny of the arguments presented in [2] would have remained undisclosed to us. We also thank anonymous referees for their constructive and useful criticism. This research has benefited from FWO Grant No. G.0115.06 for J.O.I.

## APPENDIX A: THE GIBBS ADSORPTION EQUATION

In this appendix we verify the validity of the Gibbs adsorption equation (GAE) [42] for the heuristic interface potential. The GAE relates the change in equilibrium surface free energy to a change in bulk chemical potential, the proportionality factor being the adsorption  $\Gamma$ . In our context,  $\Gamma=\Delta\rho\ell$ , for large equilibrium wetting layer thickness  $\ell$ , and the GAE takes the form

$$\frac{a^2}{k_B T} \frac{dW(\ell, H)}{dH} = \frac{\ell}{\xi}, \quad (\text{A1})$$

where we define  $W(\ell, H) \equiv V(\bar{\ell}=\ell)$  with  $V(\bar{\ell})$  as given in Eq. (29). In equilibrium,  $\ell=\ell(H)$ , determined through  $\partial V(\bar{\ell})/\partial \bar{\ell}|_{\epsilon}=0$ , so that

$$\frac{dW(\ell, H)}{dH} = \frac{\partial W(\ell, H)}{\partial H} + \frac{\partial W(\ell, H)}{\partial \ell} \frac{d\ell}{dH} = \frac{\partial W(\ell, H)}{\partial H}, \quad (\text{A2})$$

which implies that the GAE is valid. Of course, the GAE is also valid for the interface potential derived within linear RG theory.

## APPENDIX B: HYPERSCALING CONSIDERATIONS

In this appendix, we test the validity of hyperscaling (with or without logarithmic corrections) for the heuristic as well as the RG approaches. The concept of hyperscaling is concerned, in our context of wetting transitions, with the critical exponent equality

$$2 - \alpha_s^{co} = (d - 1)\nu_{\parallel}^{co}. \quad (\text{B1})$$

The exponent  $2 - \alpha_s^{co}$  characterizes the singularity in the surface free energy  $V(\ell)$  at complete wetting ( $H \rightarrow 0$ ;  $\ell \rightarrow \infty$ ), while  $\nu_{\parallel}^{co}$  is the critical exponent of  $\xi_{\parallel}$ . One expects, for interface unbinding driven by thermal fluctuations, that hyperscaling holds for  $d < d_u$ , and also at  $d = d_u$ , but in the latter case possibly with logarithmic corrections (which do not affect the exponent equality). For  $d > d_u$ , the mean-field critical exponent values for  $\alpha_s^{co}$  and  $\xi_{\parallel}$  apply and Eq. (B1) is not satisfied.

For short-range forces  $d_u = 3$  for all continuous wetting transitions and in  $d = 3$  hyperscaling predicts, in view of Eq. (B1), that the surface free-energy contribution  $V(\ell)$  vanishes in essentially the same manner as  $\xi_{\parallel}^{-2}$ . The heuristic ansatz

Eq. (22) appears to be consistent with hyperscaling, but let us calculate the behavior of the various terms in  $V(\ell)$  implied by taking  $\bar{\ell} = \ell$  in Eq. (31), and approaching complete wetting. We first note that the mean-field critical exponents are  $\alpha_s^{co} = 1$ , with logarithmic correction, and  $\nu_{\parallel}^{co} = 1/2$ , without logarithmic correction. For an interface potential of the form Eq. (31) the divergence of  $\ell$  at complete wetting obeys

$$\ell/\xi \sim \kappa^{-1} \ln(1/H) + \kappa^{-1} \ln \ln(1/H), \quad (\text{B2})$$

and

$$\frac{\gamma}{\xi_{\parallel}^2} \sim \frac{\kappa^2}{4\pi\xi^2} H, \quad (\text{B3})$$

which implies  $\nu_{\parallel}^{co} = 1/2$ , without logarithmic correction. The surface free-energy singularity follows from

$$V(\ell)a^2/k_B T \sim \kappa^{-1} H \ln(1/H), \quad (\text{B4})$$

implying  $\alpha_s^{co} = 1$ , with logarithmic correction. We conclude that hyperscaling is satisfied, but only up to a logarithmic correction factor. Such corrections are usually to be expected at  $d_u$ , but it does not make sense to discuss them within the heuristic approach, because its self-consistency does not extend far enough to control them.

The RG approach, on the other hand, satisfies hyperscaling with logarithmic corrections. Specifically,  $\nu_{\parallel}^{co} = 1/2$ , without logarithmic correction, and  $\alpha_s^{co} = 1$ , with logarithmic correction (as was the case for the heuristic approach). Note that the RG results for short-range critical wetting in  $d = 3$  satisfy hyperscaling without logarithmic corrections [28].

- 
- [1] H. N. W. Lekkerkerker, V. W. A. de Villeneuve, J. W. J. de Folter, M. Schmidt, Y. Hennequin, D. Bonn, J. O. Indekeu, and D. G. A. L. Aarts, *Eur. Phys. J. B* **64**, 341 (2008).
- [2] Y. Hennequin, D. G. A. L. Aarts, J. O. Indekeu, H. N. W. Lekkerkerker, and D. Bonn, *Phys. Rev. Lett.* **100**, 178305 (2008).
- [3] P.-G. de Gennes, *Rev. Mod. Phys.* **57**, 827 (1985).
- [4] S. Dietrich, in *Phase Transitions and Critical Phenomena*, edited by C. Domb and J. L. Lebowitz (Academic, New York, 1988), Chap. 1, Vol. 12.
- [5] D. Bonn, J. Eggers, J. O. Indekeu, J. Meunier, and E. Rolley, *Rev. Mod. Phys.* **81**, 739 (2009).
- [6] C. Hertlein, L. Helden, A. Gambassi, S. Dietrich, and C. Bechinger, *Nature (London)* **451**, 172 (2008).
- [7] M. Dijkstra, J. M. Brader, and R. Evans, *J. Phys.: Condens. Matter* **11**, 10079 (1999).
- [8] S. Asakura and F. Oosawa, *J. Chem. Phys.* **22**, 1255 (1954).
- [9] S. Asakura and F. Oosawa, *J. Polym. Sci., Polym. Phys. Ed.* **33**, 183 (1958).
- [10] A. Vrij, *Pure Appl. Chem.* **48**, 471 (1976).
- [11] B. Götzelmann, R. Evans, and S. Dietrich, *Phys. Rev. E* **57**, 6785 (1998).
- [12] B. Götzelmann, R. Roth, S. Dietrich, M. Dijkstra, and R. Evans, *Europhys. Lett.* **47**, 398 (1999).
- [13] D. G. A. L. Aarts, M. Schmidt, and H. N. W. Lekkerkerker, *Science* **304**, 847 (2004).
- [14] D. G. A. L. Aarts, R. Tuinier, and H. N. W. Lekkerkerker, *J. Phys.: Condens. Matter* **14**, 7551 (2002); G. J. Fleer and R. Tuinier, *Adv. Colloid Interface Sci.* **143**, 1 (2008).
- [15] N. F. Carnahan and K. E. Starling, *J. Phys. Chem.* **51**, 635 (1969).
- [16] D. G. A. L. Aarts, R. P. A. Dullens, D. Bonn, R. van Roij, and H. N. W. Lekkerkerker, *J. Chem. Phys.* **120**, 1973 (2004).
- [17] Y. Vandecan and J. O. Indekeu, *J. Chem. Phys.* **128**, 104902 (2008).
- [18] R. Evans, *Adv. Phys.* **28**, 143 (1979).
- [19] J. M. Brader and R. Evans, *Europhys. Lett.* **49**, 678 (2000).
- [20] J.-P. Hansen and I. R. McDonalds, *Theory of Simple Liquids*, 2nd ed. (Academic, London, 1990).
- [21] W. K. Wijting, N. A. M. Besseling, and M. A. Cohen Stuart, *Phys. Rev. Lett.* **90**, 196101 (2003).
- [22] E. M. Blokhuis, J. Kuipers, and R. L. C. Vink, *Phys. Rev. Lett.* **101**, 086101 (2008).
- [23] L. Mandelstam, *Ann. Phys.* **41**, 609 (1914).
- [24] F. P. Buff, R. A. Lovett, and F. H. Stillinger, *Phys. Rev. Lett.* **15**, 621 (1965).
- [25] For a review, see M. E. Fisher, *J. Chem. Soc., Faraday Trans. II* **82**, 1569 (1986).
- [26] R. F. Kayser, J. W. Schmidt, and M. R. Moldover, *Phys. Rev. Lett.* **54**, 707 (1985).

- [27] E. Brézin, B. I. Halperin, and S. Leibler, *Phys. Rev. Lett.* **50**, 1387 (1983).
- [28] D. S. Fisher and D. A. Huse, *Phys. Rev. B* **32**, 247 (1985).
- [29] D. Bonn and D. Ross, *Rep. Prog. Phys.* **64**, 1085 (2001).
- [30] A. O. Parry, J. M. Romero-Enrique, and A. Lazarides, *Phys. Rev. Lett.* **93**, 086104 (2004).
- [31] T. Kerle, J. Klein, and K. Binder, *Phys. Rev. Lett.* **77**, 1318 (1996).
- [32] A. O. Parry and R. Evans, *Phys. Rev. Lett.* **64**, 439 (1990); *Physica A* **181**, 250 (1992).
- [33] T. Kerle, J. Klein, and K. Binder, *Eur. Phys. J. B* **7**, 401 (1999).
- [34] R. Lipowsky, in *Random Fluctuations and Pattern Growth*, edited by H. E. Stanley and N. Ostrowsky, NATO ISI, Series E: Applied Science (Kluwer Academic, Dordrecht, 1988), Vol. 157, pp. 227–245.
- [35] M. Schick, in *Les Houches, Session XLVIII, Liquids at Interfaces*, edited by J. Charvolin, J.-F. Joanny, and J. Zinn-Justin (Elsevier, Amsterdam, 1990).
- [36] W. Helfrich, in *Les Houches, Session XLVIII, Liquids at Interfaces* (Ref. [35]).
- [37] R. Lipowsky and M. E. Fisher, *Phys. Rev. B* **36**, 2126 (1987).
- [38] E. Bertrand, D. Bonn, H. Kellay, B. P. Binks, and J. Meunier, *Europhys. Lett.* **55**, 827 (2001).
- [39] D. Bonn, E. Bertrand, J. Meunier, and R. Blossey, *Phys. Rev. Lett.* **84**, 4661 (2000).
- [40] A. J. Jin and M. E. Fisher, *Phys. Rev. B* **47**, 7365 (1993).
- [41] A. O. Parry, C. Rascon, N. R. Bernardino, and J. M. Romero-Enrique, *J. Phys.: Condens. Matter* **18**, 6433 (2006); **19**, 416105 (2007).
- [42] J. S. Rowlinson and B. Widom, *Molecular Theory of Capillarity* (Dover, New York, 2002).